Interaction of oxygen and carbon monoxide with Pt(111) at intermediate pressure and temperature : revisiting the fruit fly of surface science

Bashlakov, D.

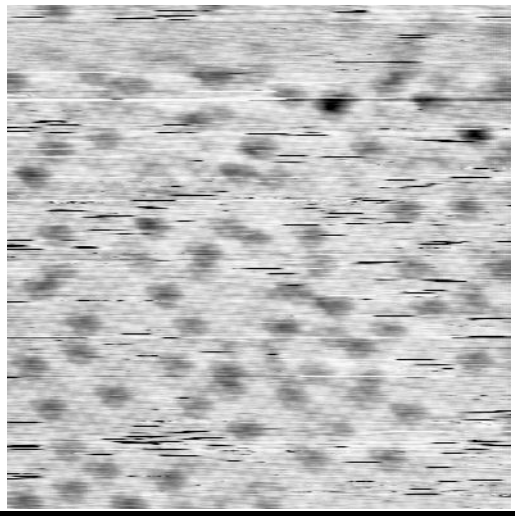

Chapter 5

Correlating surface activity and STM current transients during CO oxidation on Pt(111)

5.1 Introduction

The tremendous spatial resolution of the scanning tunneling microscope (STM) makes this technique an effective tool for surface science studies. The visualization of the surface with atomic resolution has now become routine in many laboratories [1]. Topography measurements can be seen nowadays as a conventional application of STM. At the same time, not only spatial information but also information about surface dynamics can be obtained with STM. Binning et al. were the first to demonstrate this application of STM [2]. They observed that migration of surface bound species under the tip causes a disturbance in the tunnel current. Later, it was shown that fluctuation of the tunnel current contains information on a variety of dynamic processes on the surface [3-7].

The majority of STM studies on dynamical systems have focused on the diffusion of surface bound species [6-14]. The transport of adatoms over an ordered substrate during which adsorbed species randomly jump between equilibrium adsorption sites is similar to Brownian motion. Such dynamics can be described in terms of a residence time in a single adsorption site, τ, or a hopping rate between two sites, $\nu=1/\tau$ [15]. The interest in adsorbate diffusion is caused by its importance to a number of technological processes, such as heterogeneous catalysis and epitaxial layer growth. In the case of catalysis, the ability to register each elementary step of the reaction separately may be considered as an ultimate goal for STM studies. These are adsorption, dissociation, diffusion, reaction and desorption of surface bound species.

Frame-by-frame imaging of a surface remains convenient in case of slow diffusion [8-10]. Due to the relatively long residence time of the adsorbate, its migration can be registered as the position change on two subsequent images. State of art STM systems developed in recent years are able to sample the surface with frequency of up to 100 frames per second [16, 17]. Despite this impressive performance, it remains a struggle to visualize the separate elementary steps even for a simple surface reaction such as CO oxidation [18]. Taking into account that the reaction rate for the single reaction site reaches$1x10^3$-$1x10^4$ events per second [19], the image

sampling speed should be two orders of magnitude higher for the conventional frame-by-frame approach to "see" the reaction.

An alternative approach for the study of surface dynamics is not based on visualization of atoms or molecules in space, but rather to follow them in time on a single location. The presence of adspecies causes changes in the local (electronic) density of states (LDOS), since they influence locally the electronic structure of the surface [20, 21]. Temporal changes in the LDOS due to dynamic processes cause corresponding alterations in the tip-sample tunnel barrier and changes in its conductivity (equation 2.14). Hence, motion of the surface bound species can be detected via fluctuations in the tunnel current [5, 11, 12]. It has been shown that the temporal resolution of such current fluctuation type measurements for modern STM instruments is three orders of magnitude better than the frame-by-frame method [11, 12].

Intrigued by the potential of the current fluctuation method, we have tried to apply it to CO oxidation over a platinum surface, bearing in mind that our final goal is to find the active surface sites for this reaction. Although this reaction is quite simple, it involves a number of elementary steps and each of these may be a potential source for current transients. Expecting contributions to the current fluctuations from adsorption, diffusion and recombination from both oxygen and carbon monoxide, we chose to use noise spectra of the tunnel current to quantify the current fluctuations.

5.2. Measurement approach and technique

The general thought which brought us to these noise spectra experiments is the following. Imagine two surface sites with different reactivity toward the CO+O reaction which are also continuously forming CO_2. The reactants are supplied to each site via diffusion or adsorption. The amount of CO and O arriving at the reaction site determines the reaction rate of that particular site. The latter is valid for a high gas phase-to-surface supply of the reactants. The tunnel current between surface and tip suspended over either of the two sites will vary due to the changes in LDOS of the surface during each reaction event. Figure 5.1 schematically represents such a random fluctuation of tunnel current during CO_2 formation with the reaction rate for site **II** higher than for site **I**.

We choose to use fast Fourier transformation (FFT) of the current to quantify the intensity of the current fluctuations. Figure 5.1 (c) demonstrates

the magnitude of the FFT of both I(t) traces representing the noise spectra (frequency spectra of the current fluctuations) for each site. One can see that the intensity of the noise spectrum is higher in the case of a site with higher reactivity as reaction events are more frequent. The original idea of measuring noise included collecting noise spectra at every spot of the surface while recording the surface topography. In this way we expected to obtain a reactivity map of the catalytically active surface, similar to the diffusion map obtained by Lagoute et al. on Cu(100) [7].

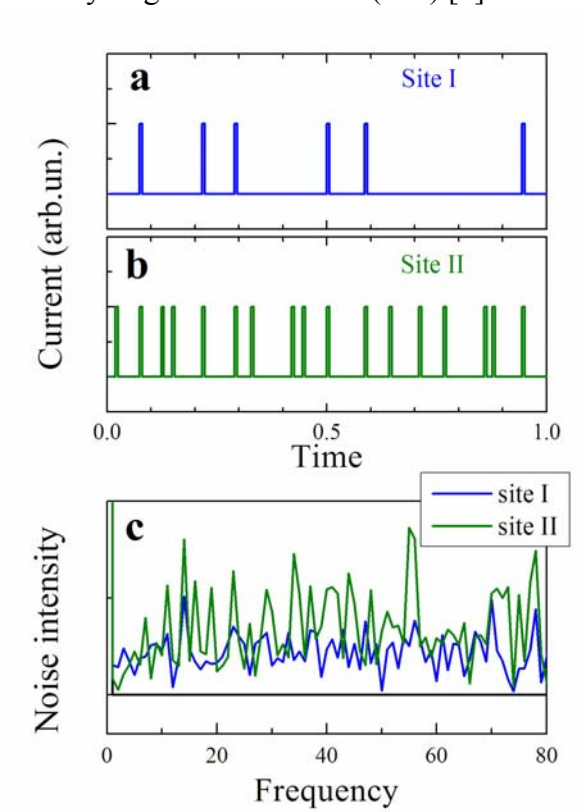

Figure 5.1 Schematic representation of the tunnel current transient during the catalytic reaction on two sites with different reactivity (a, b) and corresponding noise spectra (c) obtained by FFT of I(t) dependences.

Measurements of STM noise spectra were performed in the Omicron system (see Chapter 2 for description) by using the analysis chamber equipped with the STM stage as a closed reactor during the CO oxidation reaction. The Pt(111) sample kept at room temperature was used as the

catalytically active surface. Dosing of reactants was performed by admitting the reactant gases into the reaction chamber as is described in Chapter 4.

In order to validate the applicability of the proposed method, noise spectra were obtained while scanning the surface. For this purpose the tunnel current was sampled with a frequency of $5x10^5$ data points per second with a National Instruments DAC card (NI USB-6221 BNC). The collected array of data was converted with FFT into noise spectra. The tunnel current input for this measurement was taken from the I_{tunnel} monitor of the Omicron STM control unit. The monitored voltage of I_{tunnel} signal was obtained from the tunnel current passing via the I-V converter with 10^8 V/A conversion coefficient and was subsequently enhanced 20 times by the Preamplifier unit (last one is also the floating power supply of an I-V converter designed by Omicron). The tip height (Z) was regulated during scanning with the analog feedback loop intended to keep a constant tunnel current. It led to partial suppression of the noise spectra intensity for frequencies <200Hz. More detailed information on influence of the feedback loop on frequency spectra can be found in references 3, 7, 25, and references therein.

5.3 Experiment and results

Sets of noise spectra of the tunnel current were obtained for the Pt(111) surface exposed to carbon monoxide, oxygen and a mixture of both gases. Examples of noise spectra are shown in Figure 5.2. The broad peak in the 3-20 kHz region (pink area in Fig.5.2), which is present in each spectrum, is the characteristic feature of the I-V converter (black line). The nature of the numerous sharp peaks (best visible in the blue spectra) is not totally clear. They seem to appear as a result of parameters such as the exact way the sample is clamped in the STM stage, cars on the nearby road, walking of nearby colleagues, etc. In other words, we expect that vibrations at the system's resonant frequencies caused these peaks. They can hardly be related to dynamic processes on the surface, since similar peaks were observed while scanning the clean (bare) surface. The background noise spectrum (red line on Figure 5.2) was obtained by averaging over a number of spectra measured on the clean Pt(111) surface in separate experiments.

Noise spectra were measured on a freshly cleaned platinum surface several times to determine the noise level range in the studied system. The

tip was cleaned with the field emission treatment procedure and stabilized as described in Chapter 2 prior to every one of 9 separate runs of the background noise detection. Figure 5.2 demonstrates two of such spectra with minimum (blue) and maximum (green) noise level.

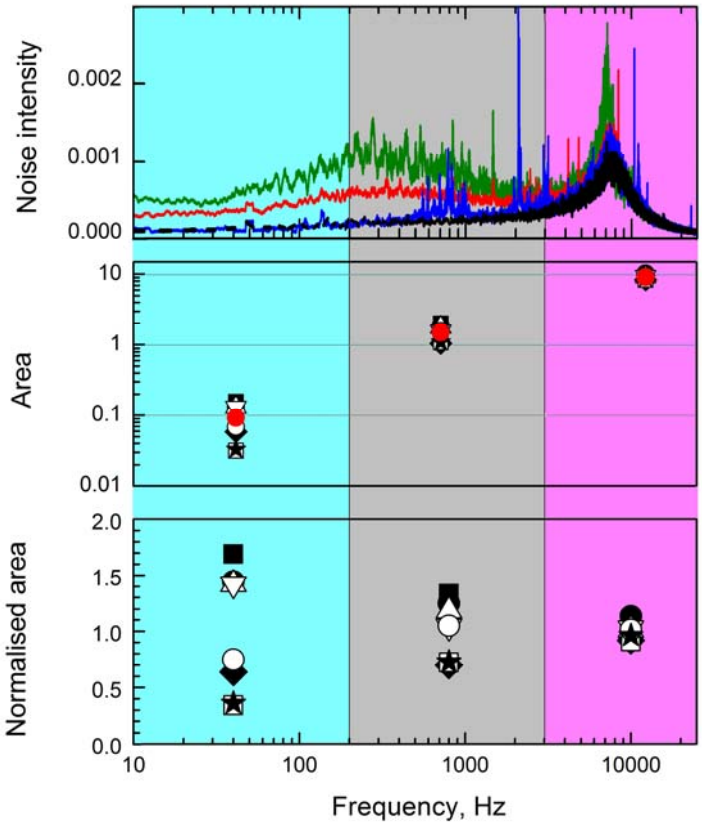

Figure 5.2 Determination of the background noise level. Top: the spectra obtained from the FFT of tunneling current: with zero current (amplifier noise – black line); lowest (blue) and highest (green) noise detected for bare platinum surface; noise spectrum averaged from 9 separate measurements (red). Middle: noise level calculated as the area under the noise spectra for 9 separate measurements (each marked with different symbol) for the frequency regions 0-200Hz (cyan), 200-3000Hz (gray) and 3-25 kHz (pink). Red symbols are an average over 9 spectra of the noise level. Bottom: deviation from the average noise level for the clean platinum surface.

The noise intensity for each spectrum was calculated as the surface area under the curve (Figure 5.2 (middle panel)). Three frequency bands were selected for analysis for the following reasons. The first band (0-200 Hz) is influenced by the feedback control of the STM electronics. Thus, the noise intensity in this region was partially suppressed. The last band (above 3 kHz) is affected by broadening of a frequency response for the I-V converter (broad peak). Only the 200-3000 Hz band seems to be unaffected by the instrument's performance. The average noise intensity was calculated for each band in order to normalize the range of the noise level of these bands. From the bottom graph of Figure 5.2 it is observed that the highest dispersion as well as the highest noise level is detected in the low frequency band, even though it is suppressed by the feedback loop.

Separate dosing of carbon monoxide and oxygen or a mixture of both gases was done to compare the noise spectra of the tunnel current without (Figures 5.3 and 5.4) and with (Figure 5.5) reaction proceeding on the surface. During carbon monoxide dosing, it was noticed that a certain period of time is needed for CO to form an ordered layer. The structure observed after this onset is shown in the right part of STM image. Scanning of this regular CO layer caused an appearance of two peaks at ≈70Hz and ≈250 Hz in the noise spectra (not shown), as a result of the delay in the feedback loop response. No other differences in the noise intensity were observed between spectra from an ordered (90-120 s) as well as a disordered CO layers (0-90 s) and the bare Pt(111) surface.

The STM images on Figures 5.3-5.6 were rotated clockwise for better representation. Unlike the previous STM images, the scan lines are now vertical. In this way the observed topographical changes can be easily compared to the time scale of the noise intensity data. The noise data are plotted as the normalized area under the noise spectra in the three frequency windows introduced in Figure 5.2 and shown as data points at the exact times at which the tunneling current datasets were collected.

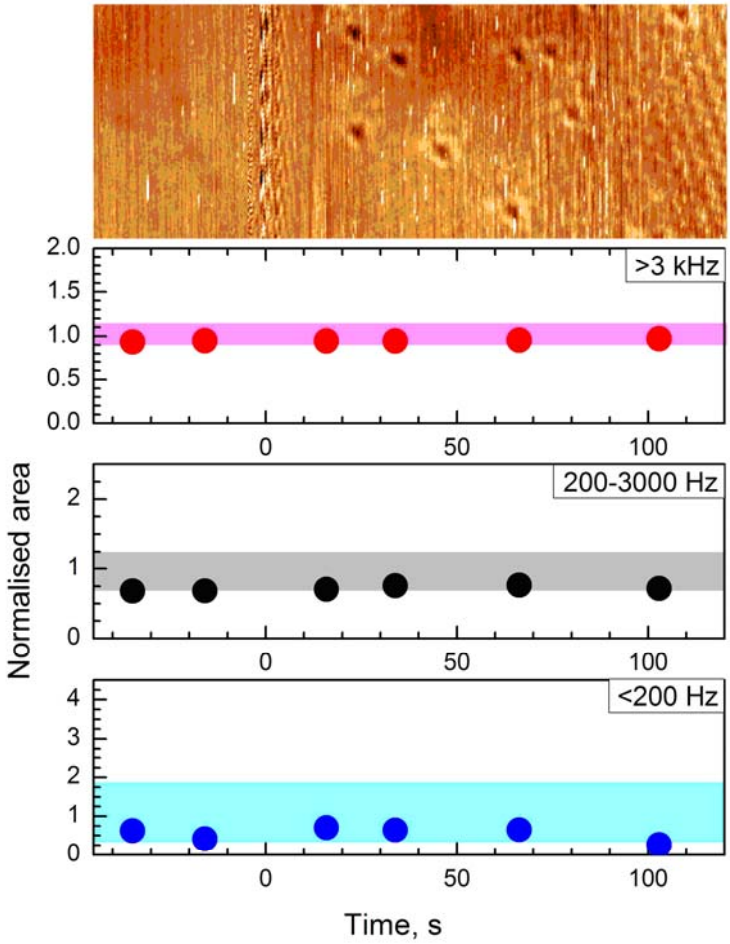

Figure 5.3 Topography of Pt(111) (17x7 nm^2, I=0.2 nA, V=0.2 V) recorded while the surface is exposed to 2-3x10^{-7} mbar of carbon monoxide. Circles show the noise level (normalized area) obtained for the three frequency windows. Bars are marking the noise level regions for the bare surface in the same frequency windows.

The dosing of O_2 at $1x10^{-4}$ mbar led to the fast formation of a p(2x2) layer of atomic oxygen as shown in the STM image in Figure 5.4. At the same time an increase in the noise intensity was observed for a number of spectra in the 0-200 and 200-3000 Hz windows. The same increase in the magnitude of the noise spectra was observed when platinum was exposed to the mixture of oxygen and carbon monoxide (Figure 5.5).

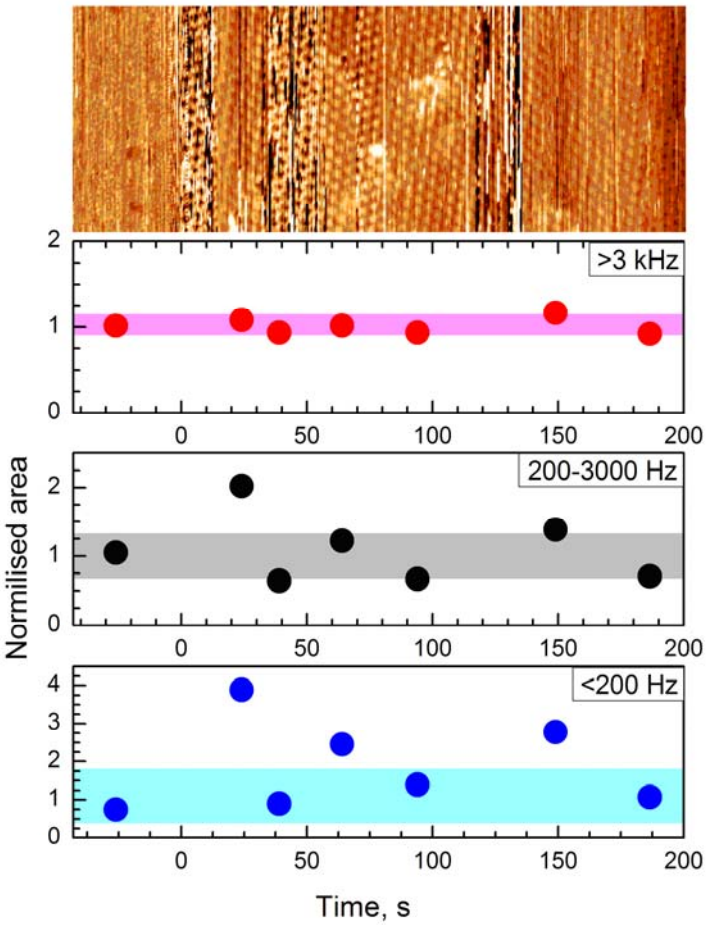

Figure 5.4 Topography of Pt(111) recorded (26x10 nm^2, I=0.2 nA, V=0.3 V) while the surface is exposed to $1x10^{-4}$ mbar of oxygen. Circles show the noise level (normalized area) obtained for three frequency windows. Bars are marking the noise level regions for the bare surface in the same frequency windows.

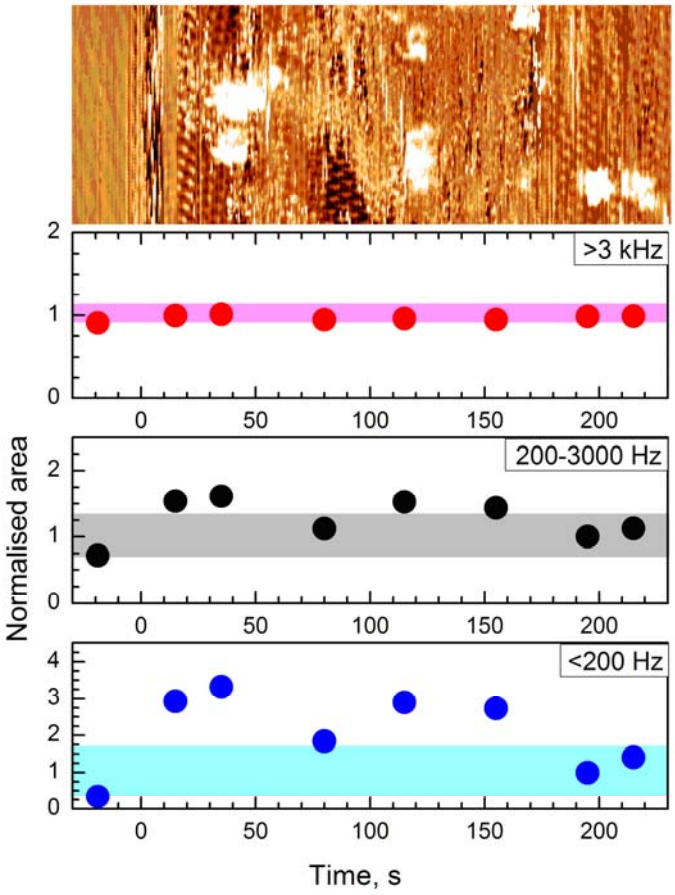

Figure 5.5 Topography of the Pt(111) recorded (26x10 nm^2, I=0.2 nA, V=0.25 V) while the surface is exposed to 1x10^{-4} mbar of the oxygen-carbon monoxide mixture (O_2:CO= 200:1). Circles show the noise level (normalized area) obtained for three frequency windows. Bars are marking the noise level regions for the bare surface in the same frequency windows.

Gold is known to be inert for oxygen adsorption at room temperature and high vacuum [22]. We employ this property to verify if the interaction of oxygen with the STM tip influences the noise spectra. Figure 5.6 shows the noise intensity variation while scanning an Au(100) surface while $1x10^{-4}$ mbar of oxygen was introduced at some point. The range of noise intensity for the gold surface-W tip was determined for the bare surface in a number of separate experiments.

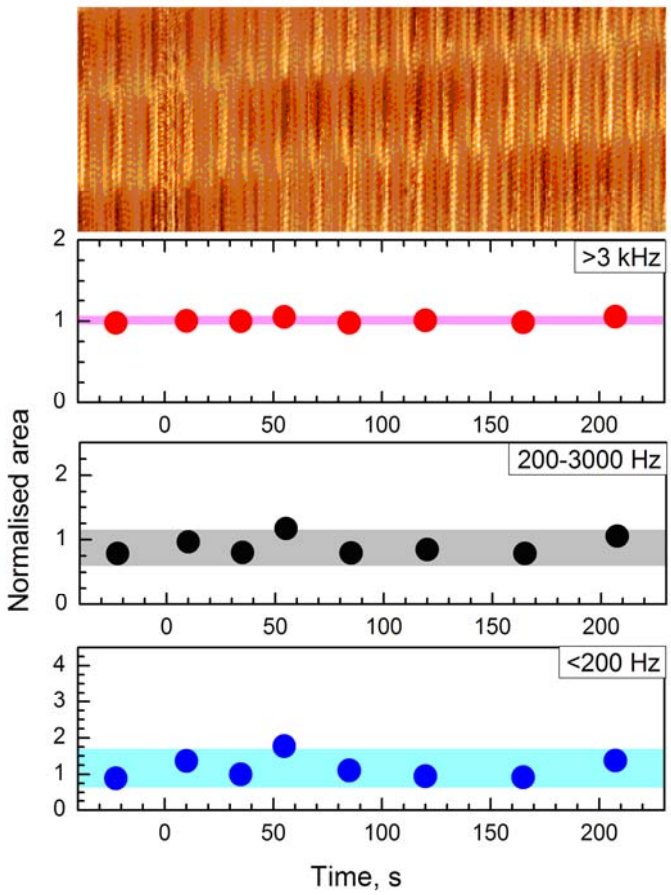

Figure 5.6 Topography of Au(100) recorded (26x10 nm^2, I=0.2 nA, V=0.3 V) while the surface is exposed to $1x10^{-4}$ mbar of oxygen. Circles show the noise level (normalized area) obtained for three frequency windows. Bars are marking the noise level regions for the bare surface in the same frequency windows.

5.4 Discussion

The interpretation of the above results is complex as there are multiple sources contributing to the current transients of the tip-sample tunnel junction. It is important to separate the influence of interfering sources such as the noise of apparatus and tip instability to extract the noise caused by dynamical processes occurring on the surface.

None of the noise spectra measured while filling the chamber with carbon monoxide revealed noticeable changes in the noise level compared to the noise spectrum produced on the clean platinum surface (Figure 5.3). At the same time, corresponding STM images show that a stable layer of CO did not form immediately after the surface was exposed to CO. Thus, there was room for diffusion of the adsorbed carbon monoxide during the initial ~90 seconds. This raises the question why the CO diffusion is not reflected as an increase in the STM noise. To anwer this question, we first note that adsorption of CO induces changes in the LDOS such that the CO molecule is seen by STM as a protrusion of 10-40 pm depending on the adsorption site [21]. We also regularly observed surface corrugation of 10-20 pm for the ordered c(4x2)-CO layer. Moreover, the noise level of our apparatus is low enough to obtain atomically resolved images of the clean Pt(111) surface with a corrugation of ≈5 pm (see for example Figure 2.4). Thus, we can exclude that a lack of spatial resolution in the *z* direction causes an apparent CO 'invisibility'. Therefore, we seek the answer in the temporal resolution of the apparatus. Extrapolating results of Wang et al. [12] to room temperature, one can obtain a hopping rate of ~100 kHz for CO migration on Pt(111). This is at least one order of magnitude higher than the bandwidth of our I-V converter (<10 kHz). Carbon monoxide is simply too mobile on Pt(111) at 300K for its diffusion to be detected in our system.

A presence of oxygen in the reaction chamber triggered an increase in the tunnel current noise level (Figures 5.4 and 5.5). Both parts of the tunnel junction, i.e. the platinum substrate and the tungsten tip, may be responsible for this. The STM image in Figure 5.4 demonstrates that the platinum surface became covered by an O-p(2x2) layer directly after oxygen was introduced at $1\text{x}10^{-4}$ mbar. Since the sticking probability of O_2 for tungsten (s_0=0.5-1 [23, 24]) is higher then for Pt(111) (s_0≈0.06), we may safely conclude that the tip was already oxidized when the noise spectra were recorded. The tungsten surface binds oxygen more strongly then platinum [15] and also hosts at least twice the amount of atomic oxygen compared to

Pt(111) [23, 24]. Therefore, we expect that fluctuations of the tunnel current are caused by the surface dynamics of oxygen on the substrate rather than processes affecting the tip. Indirect proof of this assertion is demonstrated for the gold surface, which is known to be inert towards O_2 adsorption [22]. The spectra measured on the Au(100) surface did not show an increase in the noise intensity after the chamber was filled with oxygen (Figure 5.6). However, there is no guarantee that the arrangement and nature of the tip apex was the same in the separate experiments in which measurements on the platinum and gold surfaces were done. The STM images in Figures 5.3 and 5.4 show a number of tip switching events during scanning. This indicates that changes in the LDOS of the tip apex may lead to the observed increases in noise spectra intensity.

5.5 Summary

A method using tunneling current transients to study catalytic reactions on metal surfaces was tested. Preliminary data obtained for CO oxidation gave inconclusive results regarding the applicability of this technique. The presence of CO did not affect the observed noise intensity. However, an increased intensity of current fluctuations was found when the platinum surface is exposed to oxygen and to the reactive mixture of oxygen and carbon monoxide. Although the tip instability can not be ruled out as a source of the detected current transients, the observed increase of the noise level is likely caused by the motion of the O_{ads} species on the surface, suggesting that the low O mobility is the main source of the current fluctuations both during O adsorption and during the reaction of CO with adsorbed O.

References:

[1] M. Bowker and P. D. Davies, Scanning Tunneling Micriscopy in Surface Science, Nanoscience and Catalysis, Wiley-VSH verlag GmbH & Co. KGaA, Weinheim, 2010.

[2] G. Binnig, H. Fuchs, and E. Stoll, Surface Science 169 (1986) L295.

[3] B. Koslowski, C. Baur, R. Moller, and K. Dransfeld, Surface Science 280 (1993) 106.

[4] P. A. Sloan, Journal of Physics-Condensed Matter 22 (2010)

[5] B. C. Stipe, M. A. Rezaei, and W. Ho, Physical Review Letters 81 (1998) 1263.

[6] M. L. Lozano and M. C. Tringides, Europhysics Letters 30 (1995) 537.

[7] J. Lagoute, T. Zambelli, S. Martin, and S. Gauthier, Image Analysis & Stereology 20 (2001) 175.

[8] J. Wintterlin, J. Trost, S. Renisch, R. Schuster, T. Zambelli, and G. Ertl, Surface Science 394 (1997) 159.

[9] M. O. Pedersen, L. Osterlund, J. J. Mortensen, M. Mavrikakis, L. B. Hansen, I. Stensgaard, E. Laegsgaard, J. K. Norskov, and F. Besenbacher, Physical Review Letters 84 (2000) 4898.

[10] T. Tansel and O. M. Magnussen, Physical Review Letters 96 (2006)

[11] K. Wang, C. Zhang, M. M. T. Loy, and X. Xiao, Physical Review Letters 94 (2005) 036103.

[12] K. D. Wang, F. F. Ming, Q. Huang, X. Q. Zhang, and X. D. Xiao, Surface Science 604 (2010) 322.

[13] M. Sumetskii, A. A. Kornyshev, and U. Stimming, Surface Science 307 (1994) 23.

[14] J. V. Barth, H. Brune, B. Fischer, J. Weckesser, and K. Kern, Physical Review Letters 84 (2000) 1732.

[15] J. V. Barth, Surface Science Reports 40 (2000) 75.

[16] M. J. Rost, L. Crama, P. Schakel, E. van Tol, G. B. E. M. van Velzen-Williams, C. F. Overgauw, H. ter Horst, H. Dekker, B. Okhuijsen, M. Seynen, A. Vijftigschild, P. Han, A. J. Katan, K. Schoots, R. Schumm, W. van Loo, T. H. Oosterkamp, and J. W. M. Frenken, Review of Scientific Instruments 76 (2005) 053710.

[17] F. Esch, C. Dri, A. Spessot, C. Africh, G. Cautero, D. Giuressi, R. Sergo, R. Tommasini, and G. Comelli, Review of Scientific Instruments 82 (2011) 053702.

[18] J. Méndez, S. H. Kim, J. Cerdá, J. Wintterlin, and G. Ertl, Physical Review B 71 (2005) 085409.

[19] F. Gao, S. M. McClure, Y. Cai, K. K. Gath, Y. Wang, M. S. Chen, Q. L. Guo, and D. W. Goodman, Surface Science 603 (2009) 65.

[20] F. Biscarini, C. Bustamante, and V. M. Kenkre, Physical Review B 51 (1995) 11089.
[21] M. L. Bocquet and P. Sautet, Surface Science 360 (1996) 128.
[22] S. Carabineiro and B. Nieuwenhuys, Gold Bulletin 42 (2009) 288.
[23] M. Bowker and D. A. King, Surface Science 94 (1980) 564.
[24] T. Engel, H. Niehus, and E. Bauer, Surface Science 52 (1975) 237.
[25] R. Möller, A. Esslinger, and K. Koslowski, Appl. Phys. Lett 55 (1989) 2360.